A Study on the Initial Crack Curving Angle of Isotropic/Orthotropic Bimaterial

Jai-Sug Hawong*, Dong-Chul Shin
School of Mechanical Engineering, Yeungnam University, Gyung-san City, Kyungbuk 712-749, Korea
Ouk-Sub Lee
School of Mechanical Engineering, Ihna University, Inchon 402-751, Korea

In this paper, when the initial propagation angle of a branched crack is calculated from the maximum tangential stress criterion (MTSC) and the minimum strain energy density criterion (MSEDC), it is essential that you use stress components in which higher order terms are considered and stress components at the position in a distance 0.005 mm from the crack tip (= r). When an interfacial crack propagates along the interface at a constant velocity, the initial propagation angles of the branched crack are similar to the mode mixities (phase angle) and the theoretical values obtained from MTSC and MSEDC. The initial propagation angle of the branched crack depends considerably on the stress intensity factor K_2.

Key Words : Mode Mixity, Isotropic/Orthotropic Bimaterial, Initial Crack Curving Angle, Maximum Tangential Stress Criterion, Minimum Strain Energy Density

1. Introduction

Recently, composite material is used in various engineering fields; bonding joints, bonding of metal and ceramic, and electrical devices etc.. Therefore the strength and fracture of bonding have become increasingly important. Until now, the fracture criterion of an interfacial crack has not been established, in particular the fracture criterion of a dynamic interfacial crack had not been established.

Erdogan and Sih (1963) suggested the maximum tangential stress criterion in a crack propagation angle of homogeneous material under mixed mode. Williams and Ewing (1972) experimentally studied problems of the crack propagation angle of PMMA (polymethyl metacrylate) with slanted angle. Then they compared the theoretical values of the crack propagation angle obtained from the maximum tangential stress criterion with the experimental values of the crack propagation angle. Sih (1972) introduced the criterion of the strain energy density factor, that is, the minimum strain energy density criterion. Rice (1988) suggested stress intensity factor as a fracture parameter, but he did not suggest the analytical fracture criterion as a function of stress intensity factors K_1 and K_2. He and Hutchinson (1989) suggested that the interfacial crack is propagated along the direction in which the maximum value of the energy release rate is produced. They studied the relationships between the direction of crack propagation and K_2/K_1 and between the energy release rate and K_2/K_1. Yuuki and Xu (1992) suggested an approach in which crack propagation angles could be determined by the boundary element method. In this approach, they used the maximum tangential stress criterion and material constants of bimaterial.

Most of the above analysis are studies on the initial propagation of the crack; the higher order

* Corresponding Author,
E-mail : jshawong@yumail.ac.kr
TEL : +82-53-810-2445; **FAX** : +82-53-813-3703
School of Mechanical Engineering, Yeungnam University, Gyung-san City, Kyungbuk 712-749, Korea. (Manuscript **Received** December 22, 2001; **Revised** July 25, 2002)

terms of stress function are not used. When we are going to use the maximum tangential stress criterion and strain energy density criterion to obtain the initial angle of the crack propagation, we should know the stress intensity factors and the coefficients of stress components. It is impossible to know the stress intensity factors and the coefficients of stress components in which higher order terms are considered. Therefore, in this research maximum tangential stress criterion and strain energy density criterion, in which higher order terms are considered, are used. Higher order terms are obtained from the dynamic photoelastic experimental hybrid method for the bimaterial with an interfacial crack. The relationships among the initial angle of the crack propagation, mode mixity and the optimal distance r for the initial angle of crack propagation are studied.

2. Basic Theory

2.1 Stress components in the vicinity of the crack tip propagated at a constant velocity

In the plane problems of linear elastodynamic, when the interfacial crack propagates along the interface at a constant velocity c, as shown in Fig. 1, coordinate (X, Y) is the fixed rectangular coordinate, (x, y) is the moving coordinate in which the crack tip is the original point. Eq. (1) shows the relationship between the fixed coordinates and the moving coordinates

$$y=Y,\ x=X-ct \tag{1}$$

Here, c is the velocity of the crack tip and t is the crack propagating time.

Eq. (2) gives stress components and displacement components occurring in the vicinity of the crack tip of bimaterial when the interfacial crack propagates at a constant velocity c.

$$\begin{aligned}
\sigma_{xk}&=\sum_{n=1}^{\infty}\mathrm{Re}[\lambda_n(E_{1k}M_{1kn}z_{1k}^{\lambda n-1}+\bar{E}_{1k}M_{2kn}\bar{z}_{1k}^{\lambda n-1}\\
&\quad+E_{2k}M_{3kn}z_{2k}^{\lambda n-1}+\bar{E}_{2k}M_{4kn}\bar{z}_{2k}^{\lambda n-1})\beta_n]\\
\sigma_{yk}&=\sum_{n=1}^{\infty}\mathrm{Re}[\lambda_n(F_{1k}M_{1kn}z_{1k}^{\lambda n-1}+\bar{F}_{1k}M_{2kn}\bar{z}_{1k}^{\lambda n-1}\\
&\quad+F_{2k}M_{3kn}z_{2k}^{\lambda n-1}+\bar{F}_{2k}M_{4kn}\bar{z}_{2k}^{\lambda n-1})\beta_n]\\
\tau_{xyk}&=\sum_{n=1}^{\infty}\mathrm{Re}[\lambda_n(G_{1k}M_{1kn}z_{1k}^{\lambda n-1}+\bar{G}_{1k}M_{2kn}\bar{z}_{1k}^{\lambda n-1}\\
&\quad+G_{2k}M_{3kn}z_{2k}^{\lambda n-1}+\bar{G}_{2k}M_{4kn}\bar{z}_{2k}^{\lambda n-1})\beta_n]
\end{aligned}\tag{2a}$$

$$\begin{aligned}
u_k&=\sum_{n=1}^{\infty}\mathrm{Re}[(P_{1k}M_{1kn}z_{1k}^{\lambda n}+\bar{P}_{1k}M_{2kn}\bar{z}_{1k}^{\lambda n}\\
&\quad+P_{2k}M_{3kn}z_{2k}^{\lambda n}+\bar{P}_{2}M_{4kn}\bar{z}_{2k}^{\lambda n})\beta_n]\\
v_k&=\sum_{n=1}^{\infty}\mathrm{Re}[(P_{1k}M_{1kn}z_{1k}^{\lambda n}+\bar{P}_{1k}M_{2kn}\bar{z}_{1k}^{\lambda n}\\
&\quad+P_{2k}M_{3kn}z_{2k}^{\lambda n}+\bar{P}_{2}M_{4kn}\bar{z}_{2k}^{\lambda n})\beta_n]
\end{aligned}\tag{2b}$$

where E_{ik}, F_{ik}, G_{ik}, P_{ik} $(i=1, 2)$ are coefficients of complex variables (1999), they are determined when mechanical properties of material and crack propagation velocity are determined. M_{mkn} $(m=1, 2, 3, 4)$ are coefficients of complex variables defined in the n-th eigenvalue of n-order $(=\lambda_n)$. Coefficients of complex variables depend on the physical properties of material and the velocities of the crack propagation. Therefore, they are known coefficients, λ_n is eigen value. It is also determined from the particular roots of the compatibility equation of the material and position vector. Therefore, in the Eq. (2) β_n are the only unknown variables. Eq. (3) is the dynamic stress optic law of dynamic photoelastic experiment.

$$D=\left(\frac{f_{\sigma D}N_f}{t}\right)^2=(\sigma_{x1}-\sigma_{y1})^2+4\tau_{xy1}^2 \tag{3}$$

$$\begin{aligned}
D&=\left\{\sum_{n=1}^{\infty}\mathrm{Re}\left[\lambda_n((E_{11}-F_{11})z_1^{\lambda n-1}+(\bar{E}_{11}-\bar{F}_{11})M_{21n}\bar{z}_1^{\lambda n-1}\right.\right.\\
&\quad\left.\left.+(E_{21}-F_{21})M_{31n}z_2^{\lambda n-1}+(\bar{E}_{21}-\bar{F}_{21})M_{41n}\bar{z}_{2n}^{\lambda-1})\beta_n\right]\right\}^2\\
&\quad+4\left\{\sum_{n=1}^{\infty}\mathrm{Re}\left[\lambda_n(G_{11}z_1^{\lambda n-1}+\bar{G}_{11}M_{21n}\bar{z}_1^{\lambda n-1}\right.\right.\\
&\quad\left.\left.+G_{21}M_{31n}z_2^{\lambda n-1}+\bar{G}_{21}M_{41n}\bar{z}_{2n}^{\lambda-1})\beta_n\right]\right\}^2
\end{aligned}\tag{4}$$

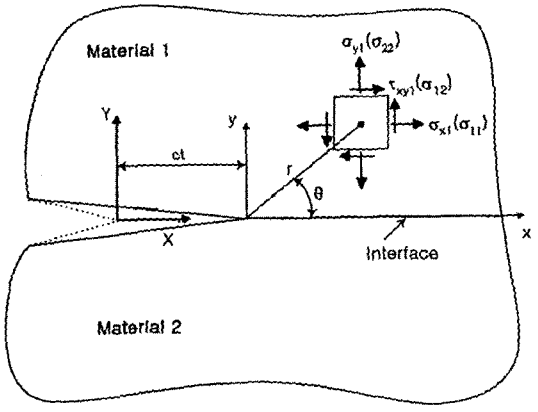

Fig. 1 Coordinate system and stress components at the crack-tip

Where $f_{\sigma D}$ is a dynamic stress fringe value and N_f is the dynamic fringe order, t is the thickness of specimen. Therefore, Eq. (4) is the function of β_n only.

Substituting experimental data measured from the dynamic photoelastic isochromatic fringe patterns into Eq. (4) and applying the concepts of non-linear least squares method to the dynamic stress optic law with experimental data, β_n can be obtained. Substituting β_n into Eq. (2), stress components and displacement components are determined, and satisfied with the given conditions. These processes are called the dynamic photoelastic experimental hybrid method for bimaterial.

The relationship between stress intensity factors and β_n is defined by eliminating the singularity of the crack tip (Aminpour, 1896). Using the definition of Aminpour, $z_{1k}=z_{2k}=r$, $n=1$ and $k=1$, Eq. (5) is obtained.

$$\begin{aligned} K_1&=\sqrt{2\pi}\ \mathrm{Re}[A_2\beta_1] \\ K_2&=\sqrt{2\pi}\ \mathrm{Re}[A_3\beta_1] \end{aligned} \tag{5}$$

where

$$\begin{aligned} A_2&=\lambda_1(F_{11}+\bar{F}_{11}M_{211}+F_{21}M_{311}+\bar{F}_{21}M_{411})\beta_1 \\ A_3&=\lambda_1(G_{11}+\bar{G}_{11}M_{211}+G_{21}M_{311}+\bar{G}_{21}M_{411})\beta_1 \end{aligned}$$

2.2 Fracture criterion of the dynamic crack

In the cracks of bimaterial the mixed modes are always produced. Most interfacial cracks of bimaterial are propagated along the interface, because the bonding strength of the interface is usually weaker than the strength of two homogenous materials.

If the bonding strength is really strong, the interfacial crack will deviate into the softer material from the interface. These cases are studied and the stress components with higher order terms are used in this paper.

2.3 Maximum tangential stress criterion

Equation (6) shows the relationships between rectangular coordinates and polar coordinates. Substituting stress components of Eq. (2a) into Eq. (6), Eq. (2a) is transformed as polar coordinates.

$$\begin{aligned} \sigma_{rk}&=\sigma_{xk}\cos^2\theta+\sigma_{yk}\sin^2\theta+2\tau_{xyk}\sin\theta\cos\theta \\ \sigma_{\theta k}&=\sigma_{xk}\sin^2\theta+\sigma_{yk}\cos^2\theta-2\tau_{xyk}\sin\theta\cos\theta \\ \tau_{r\theta k}&=(\sigma_{xk}-\sigma_{yk})\sin\theta\cos\theta+\tau_{xyk}(\cos^2\theta-\sin^2\theta) \end{aligned} \tag{6}$$

Maximum tangential stress criterion (MTSC) is that a crack propagates in the direction at which the maximum tangential stress ($\sigma_{\theta k}$) has occurred (Erdogan, 1963). Therefore, the initial angle of the crack propagation is determined from

$$\frac{\partial\sigma_{\theta k}}{\partial\theta}=0,\ \frac{\partial^2\sigma_{\theta k}}{\partial\theta^2}<0 \tag{7}$$

But, it is impossible to determine the stress components at the crack tip when r (the distance from the crack tip) is 0. There is a plastic zone in the vicinity of the crack tip. Therefore, Eq. (7) depends on the r. William and Ewing (1972) suggested that the theoretical values for the initial angle of crack propagation is corresponded with the initial angle of the fractured specimen when r is 0.05 mm. The physical meaning of r is clearly not defined until now.

2.4 Minimum strain energy density criterion

Equation (8) expresses strain energy stored per unit volume $\frac{dW}{dV}$ in the vicinity of crack tip.

$$\frac{dW}{dV}=\frac{1}{2}\sigma_{ij}\varepsilon_{ij}\quad(i,\ j=x,\ y) \tag{8}$$

where, $\varepsilon_{ij}=(u_{i,j}+u_{j,i})/2$.

Strain energy density factor(=S) is given by

$$S=r\frac{dW}{dV}=\frac{r}{2}(\sigma_x\varepsilon_x+\sigma_y\varepsilon_y+\tau_{xy}\gamma_{xy}) \tag{9}$$

Sih (1972) insisted that the fracture begins when S reaches its critical value and the crack propagates along the direction in which S takes its minimum value. The initial angle of the crack propagation in the minimum strain energy density criterion (MSEDC) is also obtained from

$$\frac{\partial S}{\partial\theta}=0,\ \frac{\partial^2 S}{\partial\theta^2}>0 \tag{10}$$

Here, it is impossible to determine the stress components at the crack tip, because there is actually a plastic zone in the vicinity of the crack tip. Therefore, to calculate Eq. (10), r is necessary. The initial angle of crack propagation depends

on the distance from the crack tip.

3. Experiment and Experimental Method

Specimens used in this research were composed of epoxy resin and aluminum plate (Al 6061) or carbon fiber epoxy composite (it is abbreviated as Ca.F.E.C) manufactured at the Korea Fiber Company. Epoxy resin is composed of matrix (Araldite) and hardner (HT-903, Ciba-Geige Co.). Their weight ratio (Araldite to hardner) is 10 to 3. They are cured through a curing cycle.

As shown in Fig. 2, half of the specimen is epoxy resin and the other half of specimen is Ca. F.E.C or aluminum.

Dimension and configuration of the specimen is shown in Fig. 2. Bonding surface of the bimaterial is cut perfectly vertical by a milling machine and is scratched by sand paper #200 to make a suitable surface roughness.

After scratching the bonding surface, the surface of two materials are cleaned by distilled water. After these processes, two materials are bonded together by epoxy adhesive. A crack is made through the teflon-molding method (Hawong, 1999) in order to make a bonding thickness less than 50 μm.

Figure 3 shows the dynamic photoelastic experimental device. The loading device has functions to which the biaxial, uniaxial dynamic or static load can be applied. The maximum strain rate of the device is 31.637 s^{-1}, that is within the resonance of the machine and structure. Controlling the oil pressure device, uniaxial or biaxial load and static or dynamic load is applied. To connect the connecting parts of the loading device with the specimen before an impact load, the mechanical synchronization is mounted on the device.

Figure 4 shows the dynamic photoelastic experimental device of the Cranz-Schardin pattern camera system (Hawong, 1999). Spark time of this system is controlled from 1 μs to 9999 μs.

Figure 5 shows the flow chart for calculating the initial angle of crack propagation and determining the optimal value of "r" using dynamic photoelastic experimental hybrid method.

1. Dynamic biaxial loading frame
2. Field lens & Polarizer & Quarter wave plate
3. Multi-spark light source
4. Multi-spark control box
5. Multi-camera 6. Load-cell 7. Accumulator
8. Dynamic amplifier 9. Oscilloscope

Fig. 3 Dynamic loading device

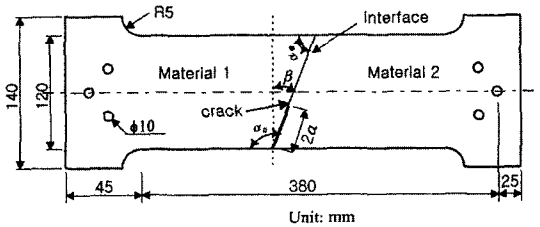

α_a: acute angle, α_o: obtuse angle, β: the slanted angle of crack
Material 1: Epoxy resin, Material 2 : Ca. F. E. C., aluminum

Fig. 2 Schematic of the specimen of bimaterial with an inclined crack

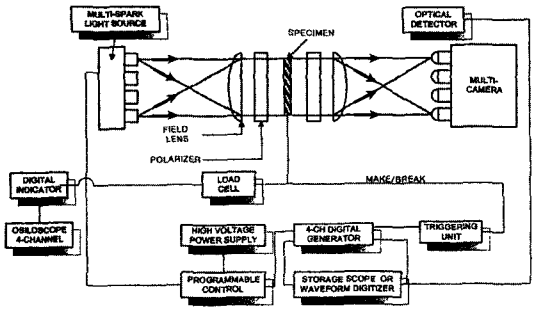

Fig. 4 Dynamic photoelastic experimental device with Cranz-Schardin pattern camera system

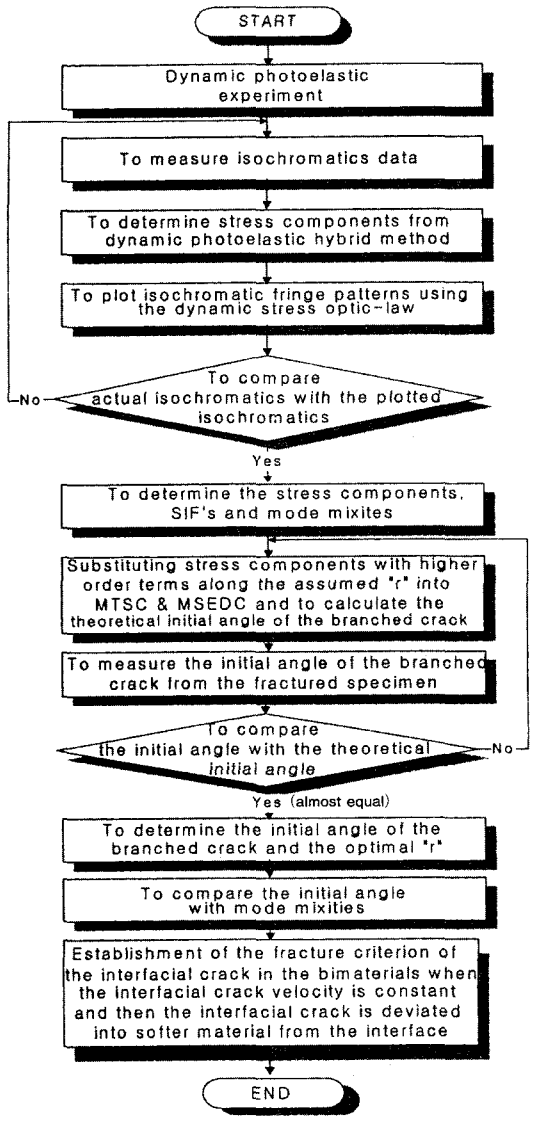

Fig. 5 Flow chart for calculating the initial angle of crack propagation and determination of optimal "r"

4. Experimental Results and Discussions

Table 1 shows the static mechanical properties of Al 6061, Carbon Fiber Epoxy Composite (Ca. F.E.C.) and epoxy resin.

Fig. 6 illustrates the isochromatic fringe patterns of bimaterial composed of epoxy resin and of Ca.F.E.C and of bimaterial with cracks along the interface in the obtuse angle part of epoxy resin. Time under isochromatic fringe patterns indicates crack propagating time after triggering.

Table 1 Properties of materials

	Ca.F.E.C.	Epoxy resin	Aluminum
$E_L(E)$ [GPa]	54.47	3.20	71
E_T[GPa]	4.63		
$G_{LT}(G)$ [GPa]	1.43	1.16	26.69
$v_{LT}(v)$	0.30	0.38	0.33
ρ[kg/m^3]	1592	1316	2770

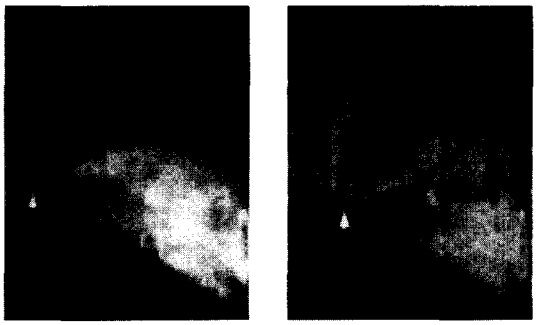

6 μ sec 54 μ sec

(a) β=30°

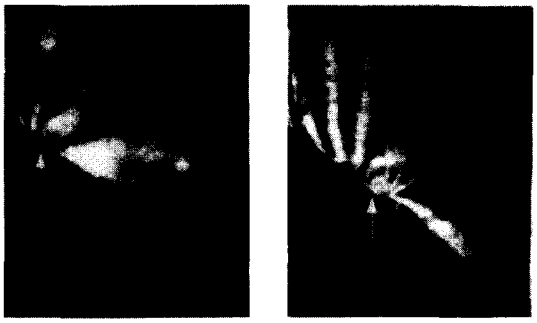

6 μ sec 54 μ sec

(b) β=45°

Fig. 6 Dynamic isochromatics of epoxy/Ca.F.E.C. bimaterial (↑ : crack-tip)

Figure 7 shows the crack propagating length with propagation time. Circular and square solid symbols respectively indicate the relationship be tween the crack propagating length and propagating time when β's are respectively 30° and 45°. In Fig. 7, the crack propagating velocities are almost constant with time. Equations (2) are stress components and displacement components when the crack propagates with a constant velocity.

Therefore Eq. (2) can be effectively used in this

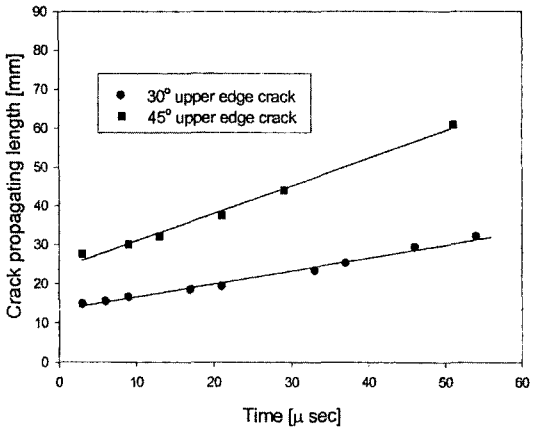

Fig. 7 Variations of crack propagating length with propagating time

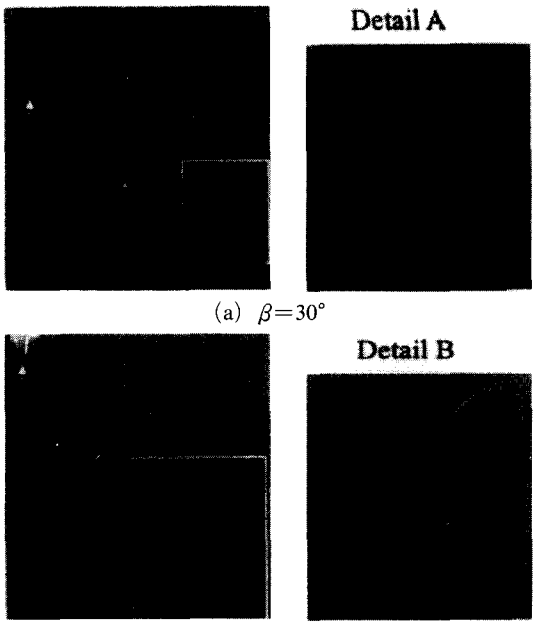

(a) $\beta=30°$

(b) $\beta=45°$

Fig. 8 Fractured specimens of epoxy/Ca.F.E.C with an edge crack in the obtuse part of epoxy resin (▲ : initial crack tip position, ↑ : propagation direction)

research.

Figure 8 reveals the fractured specimen of the bimaterial. When the slanted angle of the crack is 30°. the initial edge crack propagates along the interface and then deviates into the epoxy region with the initial angle of 77.6° from the interface at the end part of the interface.

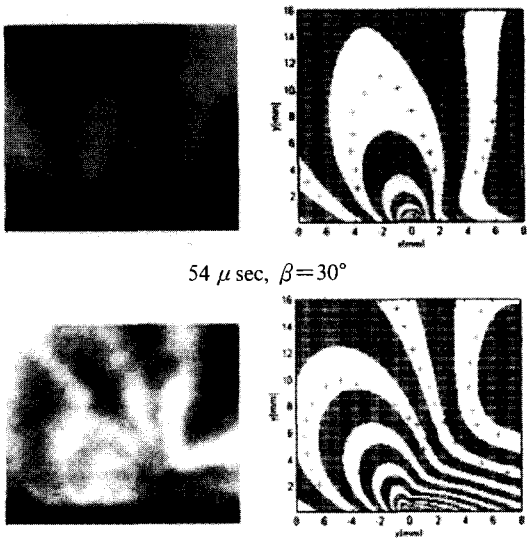

54 μ sec, $\beta=30°$

54 μ sec, $\beta=45°$

Fig. 9 Actual dynamic isochromatics and graphic isochromatics

When the slanted angle of the crack is 45°, the interfacial crack propagates along the interface and then deviates into the epoxy region from the interface. The initial angle of this crack propagation is 83.8°.

Figure 9 reveals actual isochromatics (left side) and graphic isochromatics (right side) of epoxy resin/Ca.F.E.C. bimateial. Graphic isochromatic fringe patterns are obtained from the dynamic photoelastic experimental hybrid method developed in this research. Symbol "+" indicates the positions at which experimental data are measured. As shown in Fig. 9, we can see that graphic isochromatic fringe patterns almost correspond with the actual isochromatic fringe patterns.

Figures 10 and 11(a), (b) and (c) show the contour plots of σ_x/σ_0, σ_y/σ_0 and τ_{xy}/σ_0 which are obtained from the dynamic photoelastic experimental hybrid method when $\beta=30°$ and 45° in the Fig. 9, respectively. In Fig. 10 and Fig. 11, we can see that the values of σ_y and τ_{xy} on the crack surface are zero and that they satisfy the traction free conditions.

Therefore, we can conclude that the dynamic photoelastic experimental hybrid method developed in this research is highly effective. These data are used to estimate the initial angle of crack

Table 2 Initial branched angle of epoxy/Ca.F.E.C. bimaterial with an edge crack in obtuse part of epoxy resin

Slanted angle of crack β[°]	Mode mixity ϕ[°]	Calculated initial branched angle, θ_0[°]										actual initial angle
		r=0.0001 mm		r=0.005 mm		r=0.01 mm		r=0.05 mm		r=0.1 mm		
		MTSC	MSEDC	MTSC	MSEDC	MTSC	MSEDC	MTSC	MSEDC	MTSC	MSEDC	
30	78.61	82.75	68.71	74.95	80.32	63.86	77.75	51.41	59.65	47.68	54.03	77.6
45	80.68	88.58	59.66	81.89	83.22	87.21	61.76	88.37	59.98	87.25	61.71	83.8

Note : MTSC=Maximum Tangential Stress Criterion,
MSEDC=Minimum Strain Energy Density Criterion, tan $\phi=K_2/K_1$

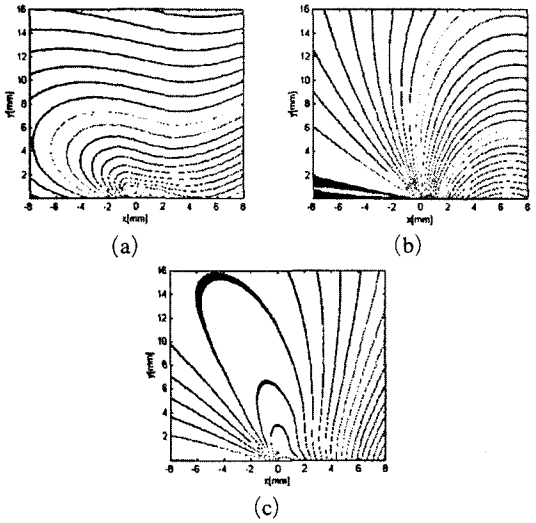

Fig. 10 Contour plots of σ_x/σ_0, σ_y/σ_0 and τ_{xy}/σ_0 obtained from the dynamic photoelastic experimental hybrid method (β=30°)

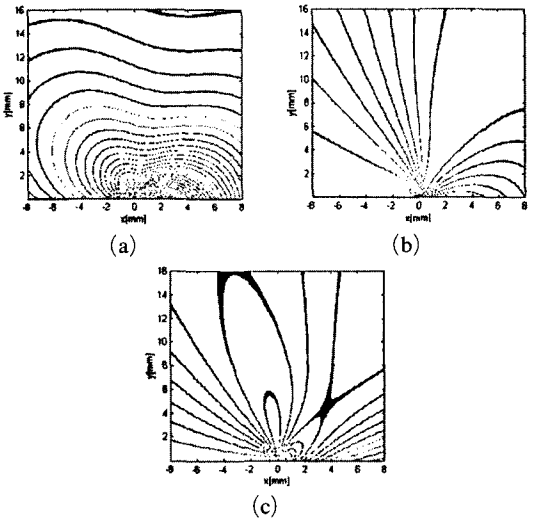

Fig. 11 Contour plots of σ_x/σ_0, σ_y/σ_0 and τ_{xy}/σ_0 obtained from the dynamic photoelastic experimental hybrid method (β=45°)

propagation.

Figure 12 indicates the normalized stress intensity factors with crack propagating time of epoxy resin/ Ca.F.E.C. bimaterial. As shown in Fig. 12, variations of stress intensity factors are very small. But, K_2/K_0 is much greater than K_1/K_0 and this is dominated by K_2. These facts indicate that the isochromatic fringe patterns are almost uniform with crack propagating time.

Figure 13 shows mode mixities with crack propagating time. As shown in Fig. 13, the mode mixities are almost constant. Mode mixities are respectively 78.6° and 80.1° when the slanted angles of the crack are respectively 30° and 45°.

Table 2 shows the theoretical values of the crack propagation initial angle with distance r from the crack tip, mode mixties and the experimental values of the crack propagation's initial angle. Theoretical values of the crack propagation's initial angle are obtained from the

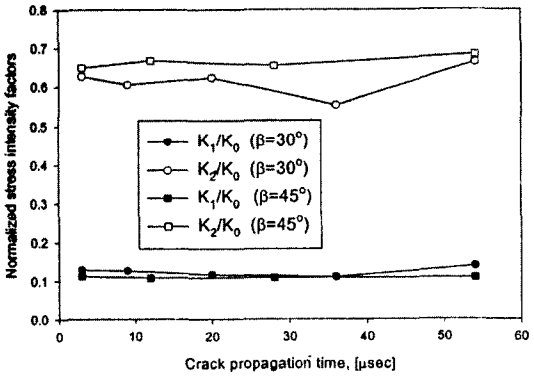

Fig. 12 Variations of dynamic stress intensity factors ($K_0=\sigma_0\sqrt{\pi a_0}$, σ_0 : initial stress, a_0 : initial crack length)

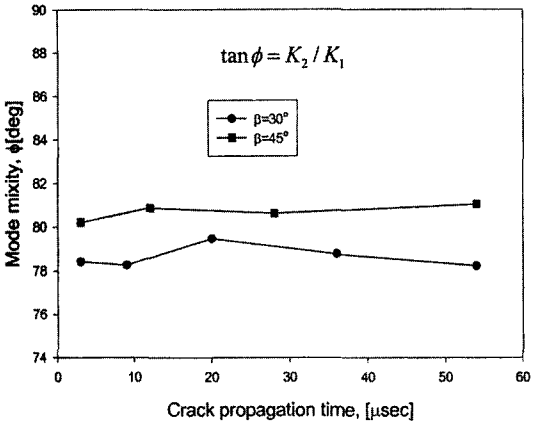

Fig. 13 Variations of mode mixity(epoxy resin/Ca. F.E.C)

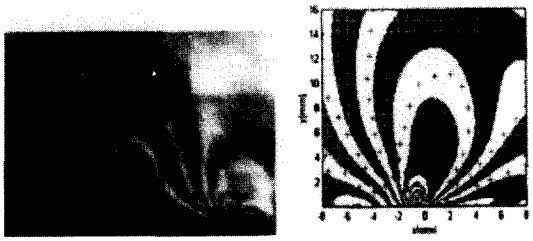

Fig. 14 Actual dynamic isochromatics and graphic isochromatics(epoxy resin/aluminum, adhesive method, crack propagation time : 27 μ sec)

maximum tangential stress criterion and minimum strain energy density criterion. Stress components obtained from the dynamic photoelastic experimental hybrid method are substituted into both criterion. It is almost impossible to take a photograph of the isochromatics produced at the moment when the crack propagates into epoxy resin from the interface.

Therefore, isochromatic data is taken from the isochromatic fringe patterns of epoxy plate which are closest to the interface of bimaterial. But, the isochromatic data can be effectively used in relation to the dynamic photoelastic experimental hybrid method, because the isochromatic fringe pattern and mode mixity are almost uniform with the crack propagating time. When r is 0.005 mm, theoretical values of the crack propagation initial angle calcualted from the MTSC and MSEDC have some differences from experimental values of crack propagation initial angles but almost correspond with them. The value r=0.05 mm which Williams and Ewing suggested is different from r=0.005 mm obtained from a numerical method considering higher order terms in this research.

In the Williams's research, higher order terms are not considered. Therefore, when the fracture criterion is studied, it is more reasonable to use the data at positions where r is 0.05 mm.

As shown in Table 2, theoretical values of MTSC almost correspond with those of MSEDC.

In the MTSC, when the slanted angles of the crack are 30° and 45° and r=0.005 mm, the theoretical initial angle of the branched crack, mode mixity, and experimental values of the branched crack etc., almost correspond with each other. In the MSEDC, when the slanted angle of the crack is 30°, they are almost identical to each other when is 0.01 mm. When the slanted angle of the crack is 45°, they are almost identical to each other when r is 0.005 mm. Through the above results, we can deduce that the theoretical values of the MSEDC are more similar to the experimental values of the initial angle of the branched crack than the MTSC. It is known through the previous results that the flow chart as shown in Fig. 5 can be effectively used to determine the initial angle of the branched crack and the optimal "r". Therefore, in this paper, processes for determining the initial angle of the crack propagation and optimal "r" are established.

Figure 14 shows actual isochromatics (left side) and graphic isochromatics (right side) of bimaterial composed of epoxy resin and aluminum plate. Graphic isochromatics is obtained from the dynamic photoelastic experimental hybrid method for bimaterial. As indicated in Fig. 14, graphic isochromatics almost corresponds with actual isochromatics, we know that the dynamic photoelstic experimental hybrid method for bimaterial is valid. In this case, as the crack propagates along the interface, propagation criterion of the initial crack can't be applied to the problem. If adhesive force between epoxy resin and aluminum is very strong, the crack will be

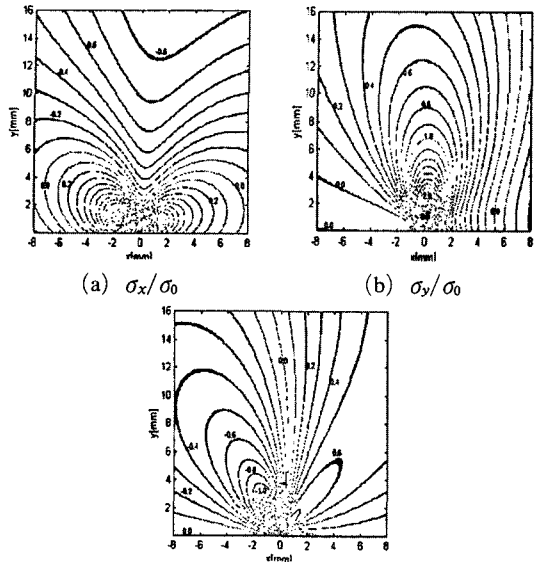

(a) σ_x/σ_0 (b) σ_y/σ_0

(c) τ_{xy}/σ_0

Fig. 15 Contour plots of σ_x/σ_0, σ_y/σ_0 and τ_{xy}/σ_0 obtained from the dynamic photoelastic experimental hybrid method (epoxy resin/aluminum, $\beta=0°$)

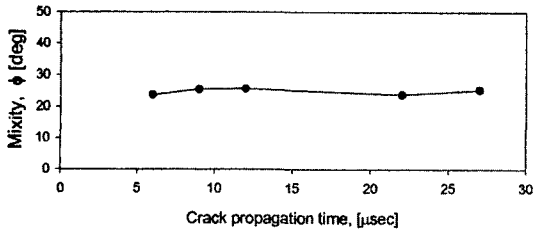

Fig. 16 Variations of mode mixity (epoxy resin/aluminum)

propagated into a softer material.

Figure 15 show the contour plots σ_x/σ_0, σ_y/σ_0 of τ_{xy}/σ_0 and which are obtained from the dynamic photoelastic experimental hybrid method in the case of Fig. 14. In Fig. 15, we can see that the values of σ_y and τ_{xy} on the crack surface are zero and that they satisfy the traction free conditions.

Figure 16 shows mode mixities with crack propagating time obtained from epoxy resin/aluminum bimaterial. As shown in Fig. 16, mode mixities are between 24° and 26°, they are almost constant.

Figure 17 shows fractured specimen of epoxy resin/aluminum bimaterial made by a molding method. In this case, adhesive force between epoxy resin and aluminum is very strong, therefore the initial angle of the branched crack is 31.4°.

Fig. 17 Fractured specimen of epoxy resin/aluminum

As shown in Figs. 16 and 17, there are some differences between 26° and 31.4°, but they are similar to each other. Mode mixity obtained from the bimaterial manufactured by adhesive method, that is, in case of Fig. 14, is 26°. The actual initial angle of the branched crack measured from the specimen made by a molding method, that is, in case of Fig. 17, is 31.4°. The differences of the initial propagation angle of the branched crack between Fig. 14 and Fig. 17 could be the result of the residual stress of Fig. 17. Therefore, it is inferred that there is a close connection between mode mixity and the initial propagation angle of the branched crack. Specifically, it is known that the initial propagation angle of the branched crack depends considerably on the stress intensity factor K_2

5. Conclusions

(1) Stress components can be determined from the dynamic photoelastic hybrid method for

bimaterial in this research. They can be effectively used in calculating the initial angle of the branched crack from the maximum tangential stress criterion and the minimum strain energy density criterion. Processes for determining the initial angle of the crack propagation and optimal "r" are established.

(2) When the initial propagation angles of the branched crack are calculated from the maximum tangential stress criterion (MTSC) and the minimum strain energy density criterion (MSEDC), one must use stress components in which higher order terms are considered and which are in a position that is 0.005 mm from the crack tip.

(3) When an interfacial crack propagates along the interface at a constant velocity and then propagates into the softer material, the initial propagation angle of the branched crack is similar to the mode mixity and the theoretical values obtained from MTSC and MSEDC. The initial propagation angle of the branched crack depends considerably on the stress intensity factor K_2.

(4) The MTSC and the MSEDC in which higher order terms are considered can be effectively used to calculate the initial propagation angle of the branched crack. But, the MSEDC is more precise than the MTSC.

Acknowledgments

The support of the Korea Science and Engineering Foundation (KOSEF) under grant number R02-2001-01135 is gratefully acknowledged.

References

Aminpour, M. A., 1986, "Finite Element Analysis of Propagating Interface Cracks in Composites," *Ph. D. Dissertation*, Univ. of Washington, Dept. of Aeronautics and Astronautics.

Erdogan, F. and Sih, G. C., 1963, "On the Crack Extension in Plates under Plane Loading and Transverse Shear," *Trans. ASME*, Dec, pp. 519~528.

Hawong, J. S., Shin, D. C., Kim, K. R. and Lee, H. J., 1999, "A Study on the Development of Dynamic Photoelastic Hybrid Method for the Fracture Mechanics of Bimaterial (Isotropic/Isotropic) Considering Residual Stress," *APCFS '99*.

He, M. Y. and Hutchinson, J. W., 1989, "Kinking of a Crack out of an Interface," *J. Appl. Mech.*, Vol. 56, pp. 270~278.

Rice, J. R., 1988, "Elastic Fracture Mechanics Concepts for Interfacial Cracks," *J. Appl. Mech.*, Vol. 55, pp. 98~104.

Sih, G. C., 1972, *Mechanics of Fracture*, Noordhoff, Leyden.

Williams, J. G. and Ewing, P. D., 1972, "Fracture under Complex Stress the Angled Crack Problem," *Int. J. Frac. Mech.*, Vol. 8, No. 4, pp. 441~445.

Yuuki, R. and Xu, J. Q., 1992, "Stress Based Criterion for an Interface Crack Kinking Out of the Interface in Dissimilar Materials," *Engr. Frac. Mech.*, Vol. 41, No. 5, pp. 635~623.